ingegneria sismica
International Journal of Earthquake Engineering
Anno XLIII - Num. 1 - 2026

Study on the Transformation of Engineering Costing Teaching in Jiangxi Red Camping Heritage: Based on the Dual Perspectives of "Historical Cost and Modern Technology".

Jianjing Zhou[1] *and LiyuanWang*[2,*]

[1] College of Modern Economics & Management, JUFE, Jiujiang, Jiangxi, 332020, China
[2] Foreign Languages School, Jiangxi University of Finance and Economics, Nanchang 310018, Jiangxi, China

SUMMARY: *A century of struggle and a century of endeavor—red heritage stands as the chronicler and witness to this grand journey and monumental struggle, serving as a living textbook for studying the history of the Party and the history of New China. In consideration of the spatio-temporal distribution and the expression form of red architecture in Jiangxi province, this paper combines a dual approach of "historical cost and modern technology." By applying the theory of quadruple helix along with digital technologies, this study seeks to develop a theoretical model for the digital transformation of red architecture in Jiangxi. Digitalized resources are included into blended learning programs for cost engineering using online learning platforms. In the process of digital transformation, UAV orthophotography creates 3D point cloud data which is processed with hierarchical thinning algorithms. Advanced registration using enhanced ICP registration technique and rotational constraint can be used for building a 3D model. Based on the above study, an experiment on blended learning was performed, where the 3D models of the red construction heritage were applied to teach engineering cost students at a university. The outcomes showed that the accuracy of the 3D models is very high, and there is a low level of discrepancy between the models and reality. In addition, the application of 3D models in the teaching process greatly improves students' academic results and learning interest.*

KEYWORDS: *Quadruple Helix Theory; Oblique Photogrammetry; Hierarchical Downsampling; ICP Point Cloud Registration; Red Architectural Heritage; Engineering Cost Education*

1 Introduction

The architectural heritage of red color is characterized by the tangible evidence of the revolutionary history of China that has been created in relation to each particular period in the development of the country's political system. The examples of the architectural heritage of the country include revolutionary bases, Long March memorial sites, the War of Resistance against Japanese Aggression, the War of Liberation, and other important revolutionary monuments created during the period of socialist construction in the country. Most of them have been converted into a new purpose from their former purpose, which included houses, ancestral halls, and temples [1-4]. With the increasing focus of the country on the issues of cultural heritage protection and inheritance, the restoration, protection, preservation, and utilization of these red

*1200600226@jxufe.edu.com
https://doi.org/10.65102/is2026131 Published: 30 April, 2026

architectural heritages have attracted significant attention in heritage protection projects, balancing both economy and history [5-7]. The issue of construction cost estimation has gained great significance because of the need for achieving the economic goals of the project, rational use of resources, and avoiding budgeting mistakes [8, 9]. It also serves as a vital tool for assessing the economic feasibility of preserving red architectural heritage [10]. Compared to the modern construction project, historical construction cost estimation shows its uniqueness. Firstly, restoration and protection will always need thorough investigation and reconstruction according to some historical documents, archives and discoveries of archaeology that requires great amounts of time and energy [11-14]. . Secondly, restoration and protection involve a combination of both construction costs and the greatest possible cultural heritage value of the buildings. Thus, this work is supposed to be done by specialists, who have enough historical experience in research [15-18]. As such, providing an innovation and transformation of the construction cost analysis from the perspective of historical cost and new technologies as the scientific way of architectural heritage protection will help to develop the construction cost science.

The red cultural heritage contains revolutionary spirit. Its conservation not only requires physical conservation but also spiritual inheritance. This paper develops a digital transformation framework for the red construction heritage of Jiangxi Province based on quadruple helix theory and taking into consideration the historical cost and new technology factors. By virtue of its geographical location and value expressions, the digital transformation framework of red construction heritage is introduced into the teaching process in blended learning mode for engineering cost management. In the case of the 3D reconstruction of red architecture heritage of Jiangxi province, this paper adopts the oblique measurement technique by drones to acquire the point clouds. Data optimization was completed with the use of hierarchical thinning method based on curvature analysis and optimized ICP algorithm with angle constraints to construct 3D models of the heritage buildings. It can be used as a teaching resource in blended learning for engineering cost estimation.

2 Pathways for Educational Transformation of Jiangxi's Red Heritage Sites

The existence of cultural heritage is proof of the advancement of civilization as well as a precious national legacy, which cannot be replicated. Preserving the cultural heritage of one’s country is an obligation as well as a high-sounding task undertaken by all of mankind. Jiangxi has a long historical past related to the war of resistance, having many revolutionary bases that have shaped unique red architecture heritages. In the context of "historical cost and modern technology," what the study of the digitalization of red architecture heritages and its application in engineering cost education in Jiangxi is all about.

2.1 Distribution and Value of Jiangxi's Red Heritage Sites

2.1.1 Spatial and Temporal Distribution of Red Construction Heritage

The red architecture legacy of Jiangxi, which is the focus of this article, began from 1922 (the Anyuan Railway Mine Workers’ Strike) until the formation of the People’s Republic of China. Because of the changing nature of revolutionary events, time development and space distribution are intricately connected regarding this architecture legacy. In general, they can be categorized into the following periods:

First Phase: The Early Workers' and Peasants' Movement Period (1922-1927). The red

architecture heritage was dispersed in places like Pingxiang, Ji'an, Ganzhou, among others, with the location where the Anyuan Railway Mine Workers' Movement occurred in Pingxiang as an example. Red buildings during this period featured aspects of industrial heritage because of the large-scale mass character of the revolution led by the Communist Party.

Phase Two: The Nanchang Uprising and Autumn Harvest Uprising Period (1927)

During this phase, military sites were the main form of red architecture, creating cultural corridors based on the paths taken by the uprising armies. The Nanchang Uprising corridor stretched from Nanchang southwards to the Jiangxi-Fujian border and then eastwards to Guangdong Province. Zhu De was leading his troops to the south in Jiangxi Province and Hunan Province, finally meeting Mao Zedong in Jinggangshan. In the Autumn Harvest Uprising corridor, there were several uprisings along the Hunan-Jiangxi border. The important locations include Xiushui, Anyuan, Tonggu, Liuyang, Wenjia, and Lianhua, with the army moving southwards to Jinggangshan. Some representative red architecture during this phase includes the Nanchang August 1st Uprising Historic Site Complex, the Pingxiang Anyuan Military Conference Historic Site, the Tonggu Xianggan Border Autumn Harvest Uprising Front Committee Historic Site, and the Yongxin Sanwan Reorganization Historic Site Complex.

Phase Three: Jinggangshan Revolutionary Base Area Period (1927-1929). Red architecture focused on Ziping with its distribution across Ninggang, Yongxin, Lianhua counties, Ji'an, Anfu, and Suixian. Important sites include Maoping Revolutionary Site Complex, Ziping Revolutionary Site Complex, and Huangyangjie Site Complex.

The fourth phase: The Soviet Area Period (1929-1934). In this phase, the Party led the people to build revolutionary base areas like Central Soviet Area, Xianggan Soviet Area, Xiang-E-Gan Soviet Area, and Min-Zhe-Gan Soviet Area in Jiangxi and other surrounding provinces with the help of revolutionary efforts. A fully developed system including Party and government structure as well as economic, cultural, educational, and health organizations was formed at all levels from central to local level, indicating the elements of a modern socialist state. Thus, in this era, although the majority of the buildings were used for the construction of the soviet areas by making use of the existing structures, a wide variety of types could be seen. Besides, there was a great deal of buildings constructed without any reference to previous ones.

Fifth Phase: The Long March and Founding of New China (1934-1949). When the Red Army began the Long March campaign in October 1934, the revolution period in Jiangxi became dormant. The remaining Red Army forces persisted in guerrilla warfare, with revolutionary sites scattered across the mountainous border regions of Jiangxi and neighboring provinces. Additionally, following the outbreak of the War of Resistance Against Japan in 1937, guerrilla units across eight southern provinces were reorganized into the New Fourth Army. The associated historical sites serve as vital physical testimonies to the Communist Party of China's anti-Japanese struggle behind enemy lines.

2.1.2 Manifestation of the Heritage Value of Red Construction Sites

Red building carries unique revolutionary history, is the material carrier of the spirit of the Long March, in the Central Soviet District and the Long March, the Communist Party of China and the Central Red Army is relying on the firm ideals and beliefs and strong revolutionary will, time and time again in desperate circumstances, the more frustrated the more courageous, and finally won the victory. As a material carrier of spiritual culture, red buildings inspire future generations to remember the spirit of the Long March and move forward. As the consolidated rear base of the Central Soviet Area, which has made great contributions to the Chinese revolution, red buildings, in the role of red cultural carrier, convey the Long March spirit of hard struggle and indomitable to the descendants [19].

The Long March of the Central Red Army is an epic that has been recorded by the history

of both the Chinese Communist Party and Chinese Workers' and Peasants' Red Army as a unique story within the scope of modern Chinese history and military history across the globe. In this case, the Long March left us the precious legacy of the spirit of the Long March, while the historical relics, which represent those red buildings, possess significant educational value for inheriting this invaluable heritage. By researching the historical relics, we can conduct patriotic education activities and thereby help people think more about history and deeply appreciate the tremendous sacrifice that revolutionaries have made in achieving national liberation and freedom. This will encourage future generations to forge ahead with unshakable determination and work hard to develop socialism with Chinese characteristics and realize the Chinese dream of revival.

2.2 Teaching Transformation Pathways for Red Heritage Project Cost Estimation

2.2.1 The Basic Model of the Quadruple Helix Theory

With economic and social developments, it is increasingly evident that the traditional social production models represented by the triple helix theory have become inadequate for addressing the needs of contemporary society. Table 1 demonstrates the features of the three social production models. In today's environment of increasing social competition where resource limitations are increasingly critical, Production Models I and II lag behind the innovation-driven production model featuring multiple systems.

Table 1: Three social production models

Production mode	Operating entity	Operation mode	Dynamic mechanism	Production characteristics
I	Single subject	Dot linear	Single double screw	Meet single demand
II	Cross-domain and multilevel body	Nonlinearity	Triple screw	Meet the needs of social innovation
III	Multi-layer, multiform, multi-node, multi-system group of multilateral systems	Multidimensional network	Four screws	The innovation of social and public interests is developed and coordinated

In comparison to the first two models, the model of social production that relies on the quadruple helix process of multi-stakeholder collaboration in development shows more innovation and dynamism. As compared to other models, the model of social production that incorporates the concept of sustainable development involves a multi-level, multi-form, and multi-node development model wherein different clusters interact in terms of mutual reinforcement and complementation. This development model is known for its higher levels of stability, innovation, and sustainability.

2.2.2 Transformation Framework for Digital Collaboration

One of the essential trends in the process of preservation and communication of red architectural heritage in the digital era is that of digitization. The concept of digitization of red architectural heritage includes the employment of advanced digital technologies, including digital acquisition, storage, processing, presentation, and communication, to convert and restore such

heritage into digital form that can be communicated, preserved, interpreted, and utilized in innovative ways. The process of red architectural heritage digitization is a multi-faceted systematic effort and an investment- and technology-intensive industry. It is not feasible to be accomplished merely through cultural institutions' efforts; rather, it necessitates collaborative and co-creative effort from multiple participants, involving cultural institutions, academe, industry, and governmental organizations. In light of the double lens of "the cost of history and modern technologies," this paper employs the quadruple helix framework in developing the collaboration framework for digitalization of red architecture heritage in Jiangxi. The proposed framework includes various stakeholders such as government agencies, industries, higher learning institutions, and citizens, as shown in Figure 1 below.

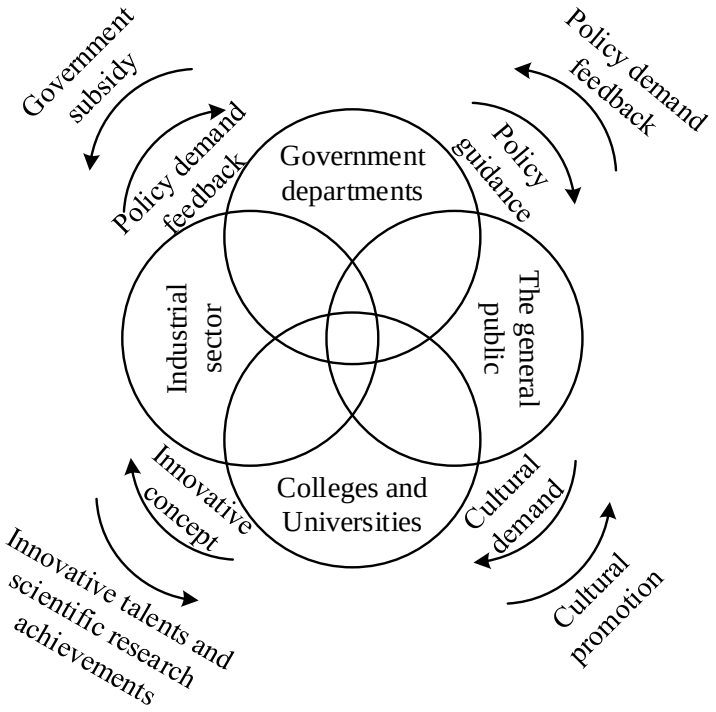

Figure 1: The transformation framework of digital collaboration

Government Departments—Policy Guidance and Financial Support. The government departments act as major forces driving and regulating the process of the digitalization of red architecture heritage in Jiangxi Province by aligning the value aspirations of industrial sectors, universities, and the public.

Industrial Sectors—Product Development and Operations. Major organizations including cultural organizations and departments responsible for cultural industries should adhere to the policies set out by the government and fulfill the demand by the public regarding the red architecture heritage. These institutions need to communicate to the universities any technological requirements for digitizing the heritage as quickly as possible.

Universities and Research Institutions—Talent Development and Technology Transfer. Universities and research organizations are the main forces that drive technological innovation in the field of red architecture heritage digitization. These organizations follow the decisions made by the government and offer talent development and technology transfer solutions to the industries and spread awareness regarding the cultural heritage among the public.

The Public—Active Participation in Cultural Promotion. The general public is an active participant and supervisor in the digitalization process of red architecture heritage.

2.2.3 Pathways for Teaching Transformation in Engineering Cost Management

The Engineering Cost Estimation module is designed to teach students basic principles and techniques of measuring and cost estimation to prepare bills of quantities and prices. Integrating the red construction heritage of Jiangxi into engineering cost education not only instills in the students a red culture spirit but also helps them understand the unique structures of these constructions in detail, which will help them learn bill of quantities for various structures, thereby improving their skills in engineering cost management. Moreover, the digitization of the red construction heritage of Jiangxi offers new possibilities for cost engineering education. By uploading the digitalized model of the red construction heritage of Jiangxi on educational websites, students can view its structure from various angles, which will help improve their skills in cost engineering.

In conclusion, this paper proposes a blended learning model using 3D models of red architectural heritage in Jiangxi, as depicted in Figure 2. Lecturers can effectively integrate these 3D models and upload them on learning websites, helping students identify architectural parts. In addition, question-and-answer sessions via online discussion forums will allow teachers to detect common problems and enhance their lesson plans and teach accordingly.

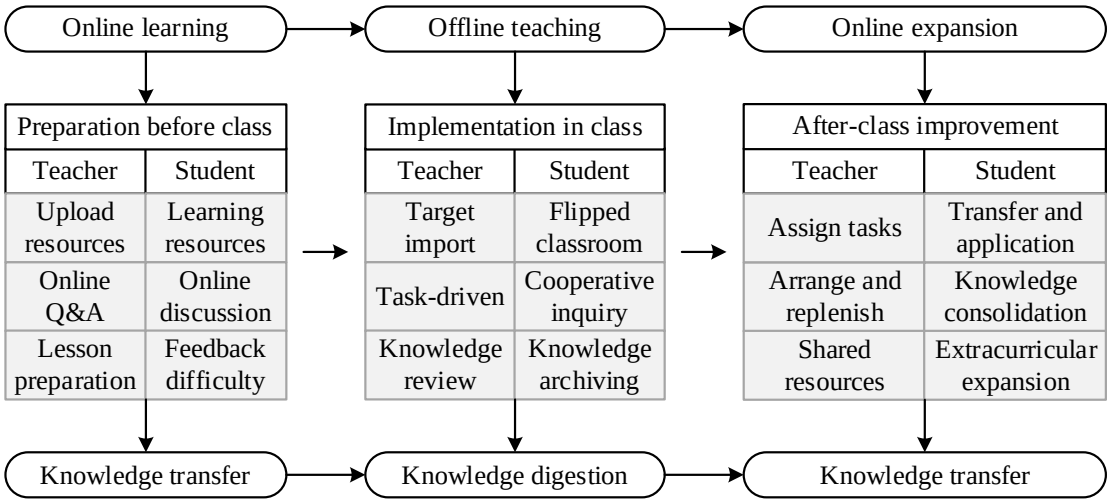

Figure 2: Blended teaching model

(1) Pre-class Phase. It is essential that during the preparatory process, the instructor utilizes information technology to create an online learning environment for the students with a clearly identified goal, substantive richness, and flexible structure. Careful consideration has to be paid when selecting the teaching resources since the teacher should take into account the characteristics of their cognition and knowledge about the subject and carefully choose appropriate and relevant multimedia that can enrich their understanding of the topic through the use of industry-related cases.

(2) In-Class Phase. Project-based Learning to Enhance Skills in-class sessions should primarily focus on the “project-task driven plus multimedia-assisted teaching” approach to guide the students to conduct deep exploration and skills training for the Jiangxi Red Construction Heritage Project.

(3) Post-class activities. The post-class activities of localized blended learning go beyond homework assignment and develop a systematic “feedback-evaluation-guidance-optimization” model committed to guaranteeing effective learning results for every learner.

3 Three-Dimensional Modeling of Jiangxi's Red Heritage Sites

In this modern age where digital technologies are advancing at an unprecedented speed, current methods are being used to convert Jiangxi's architectural heritages in digital formats by taking into account their historical costs. This chapter will largely apply the drone oblique measurement technology to collect three-dimensional point cloud data of the architectural heritage of Jiangxi. A three-dimensional model of the architectural heritage can be made using the point cloud thinning and registration technique. On the basis of this model, digital teaching materials can be created.

3.1 Oblique Photogrammetry Technology and Detailed Modeling Workflow

3.1.1 Technical Characteristics of Oblique Photogrammetric Modeling

The technique of oblique photogrammetry was developed from traditional photogrammetry techniques by improving their limitation of acquiring images from only vertical angles. With multiple sensors used in the acquisition process, information is acquired very quickly and efficiently, and it precisely represents the ground situation. Thus, 3D models created using oblique images are much closer to reality and more realistic to human eyes. Photography equipment that uses POS (Positioning, Orientation and Surveillance) system allows simultaneous collection of imagery along with spatial location and orientation information of the camera at the time of image collection. This results in the availability of rich geographic information with reduced costs for 3D modeling [20]. The key features of oblique photogrammetry using UAVs include:

(1) UAVs are used at comparatively lower heights making high resolution images possible. In addition, their camera setups allow complete coverage of ground situations, both top and side views.

(2) It involves low cost operations due to use of UAVs with reduced labors and materials as well as lesser time taken.

(3) Its modeling process is automated, easy and fast, producing accurate results equivalent to surveying quality.

3.1.2 Process Design for Detailed Modeling

After obtaining the spatial 3D information of the building through drone oblique photogrammetry, refinement of the model is required to maintain its visual quality and completeness. Hence, this paper investigates techniques that may be used to refine the real-world 3D model through geometric structure repair, texture repair, individual object reconstruction, and full repair. The workflow for such purpose includes:

(1) Performing standard aerial surveying activities within the survey area, making sure that the suitable ground control points are established to satisfy aerial overlap conditions. Going through processes like aerial triangulation, dense matching, and model reconstruction results in an unrefined real-world 3D model.

(2) Refining the 3DM through rectification of geometric and textural distortions.

(3) Resolving major texture clipping and structure deformations for buildings by means of individual object reconstruction.

(4) Carrying out full repairs, including the deletion of small floating objects and water surface repairing.

This process flow is depicted in Figure 3 below.

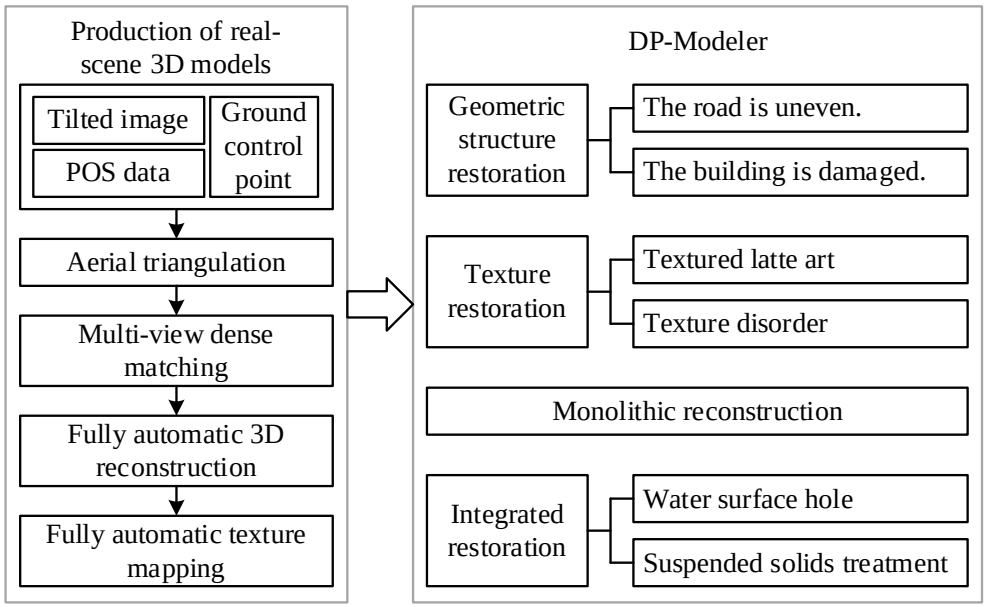

Figure 3: Refined modeling flowchart

3.2 Point Cloud Fine Registration Algorithm and 3D Modeling

3.2.1 Hierarchical Thinning Method for 3D Point Clouds

Point cloud thinning is a common method for simplifying point cloud data. The voxel subsampling algorithm creates a 3D voxel grid from the input point cloud data. Within each voxel, the centroid of all points in that voxel approximates the display of other points within it, thereby replacing multiple points with a single point to achieve thinning. The sparsification ratio is controlled by adjusting the voxel range size. A larger range parameter results in a higher sparsification ratio, while a smaller range parameter yields a lower sparsification ratio. This sparsification method enables varying sparsification levels tailored to different point clouds.

Given a non-empty voxel V containing m points, the voxel's centroid P can be expressed using coordinate information as:

$$P_{centroid} = \begin{cases} x_{centroid} = \dfrac{\sum_{i=1}^{m} x_i}{m} \\ y_{centroid} = \dfrac{\sum_{i=1}^{m} y_i}{m} \\ z_{centroid} = \dfrac{\sum_{i=1}^{m} z_i}{m} \end{cases} \tag{1}$$

While overall simplification of point clouds can address the issue of massive point cloud data volumes, the simplification process also reduces detailed features in the model. Therefore, global point cloud simplification lacks specificity. Instead, different point cloud forms should

employ corresponding simplification methods—namely hierarchical thinning—to achieve efficient point cloud simplification. For point cloud hierarchical classification, this paper proposes a method utilizing curvature values to classify point clouds. Surface curvature values are computed for the point cloud. Based on the magnitude of these curvature values, inverse constraints are formed to calculate the proportion of points within different curvature value ranges. By comparing the point cloud proportions across various curvature thresholds, hierarchical classification is achieved. Using the curvature proportion at each threshold, curvature values exhibiting significant proportion increases and clear class transitions are selected as classification criteria for the point cloud.

The radius range r of neighborhood search during curvature calculation is a critical factor influencing the outcome. Adjusting the radius r affects the sensitivity and locality of curvature computation: a smaller radius yields a narrower search range and more detailed curvature calculations, while a larger radius expands the search range and produces coarser curvature estimates. Setting an appropriate search range r helps highlight detailed features.

The search radius r in k-nearest neighbor search is typically expressed as the radius of a spherical region centered at the target point. Mathematically, this spherical region can be denoted as $B(p,r)$, where p is the center point (target point) and r is the radius. Thus:

$$B(p,r) = \{q \mid d(p,q) \le r\} \tag{2}$$

Here, $d(p,q)$ denotes the distance between points p and q, while $B(p,r)$ represents the spherical region centered at p with radius r, encompassing all points q satisfying $d(p,q) \le r$.

The larger the value of the curvature of the surface of a point cloud, the greater the variation of its shape in the vicinity of that point. In point clouds, the curvature of a point is usually calculated based on the angle formed between the normal vectors within its local neighborhood. The curvature of the surface within the neighborhood region will be large when the surface has a lot of change, otherwise, it will be small.

Let the eigenvalues of the covariance matrix be $\lambda_1, \lambda_2, \lambda_3$, where $\lambda_1 \ge \lambda_2 \ge \lambda_3$. The curvature value is calculated as follows:

$$curvature = \frac{\lambda_3}{\lambda_1 + \lambda_2 + \lambda_3} \tag{3}$$

3.2.2 Rotation Angle Constrained ICP Point Cloud Registration

Point cloud registration is an important link in three-dimensional modeling, which usually consists of two phases: coarse registration and fine registration. The aim of coarse registration is to minimize the difference between the two initial point clouds in terms of rotation and translation [21]. The commonly used Iterative Closest Point (ICP) method incurs substantial computational overhead and demands high hardware specifications when processing large datasets. Therefore, this paper proposes an improved ICP method incorporating rotational angle constraints for point cloud registration. First, upper and lower bounds for the rotational angle are estimated using optimal matching criteria to establish a registration model. Subsequently, the improved ICP algorithm is applied to perform point cloud registration.

Point cloud registration based on bounded rotation angles can be described as follows:

$$\begin{cases} \min \sum_{i=1}^{n} \| (Rm_i + t) - d_{c(i)} \|^2 \\ R^T R = I_n, \det(R) = 1 \\ \theta_x \in [\theta_{xb} - \Delta\theta_x, \theta_{xb} + \Delta\theta_x] \\ \theta_y \in [\theta_{yb} - \Delta\theta_y, \theta_{yb} + \Delta\theta_y] \\ \theta_z \in [\theta_{zb} - \Delta\theta_z, \theta_{zb} + \Delta\theta_z] \end{cases} \tag{4}$$

Among these, $R = R_x R_y R_z$. That is:

$$R_x = \begin{vmatrix} 1 & 0 & 0 \\ 0 & \cos\theta_x & -\sin\theta_x \\ 0 & \sin\theta_x & \cos\theta_x \end{vmatrix}, R_y = \begin{vmatrix} \cos\theta_y & 0 & \sin\theta_y \\ 0 & 1 & 0 \\ -\sin\theta_y & 0 & \cos\theta_y \end{vmatrix}_z = \begin{vmatrix} \cos\theta_z & -\sin\theta_z & 0 \\ \sin\theta_z & \cos\theta_z & 0 \\ 0 & 0 & 1 \end{vmatrix} \tag{5}$$

In the equation, $\theta_x, \theta_y, \theta_z$ are the rotation angles, $\theta_{xb}, \theta_{yb}, \theta_{zb}$ are the mean rotation angles, $\Delta\theta_x, \Delta\theta_y, \Delta\theta_z$ are the rotation angle deviations, $\theta_{xb} - \Delta\theta_x, \theta_{yb} - \Delta\theta_y, \theta_{zb} - \Delta\theta_z$ are the lower bounds of the selected rotation angles, and $\theta_{xb} + \Delta\theta_x, \theta_{yb} + \Delta\theta_y, \theta_{zb} + \Delta\theta_z$ are the upper bounds of the rotation angles.

After incorporating rotation angle constraints, the specific implementation steps of the improved ICP method are as follows:

(1) Estimate the boundaries of the three rotation angles.

(2) Set the initial transformation R_0 and t_0, define $M_0 = R_0 M + t_o$, and set the iteration count k=0.

(3) Set k=k+1 and establish the relationship: $c_k(i) \in \{1, 2, \cdots, n\}$.

(4) Compute $\theta_{x0}, \theta_{y0}, \theta_{z0}, R = R_{x0} R_{y0} R_{z0}$, and $t_k = \frac{1}{n}\left(-R_k \sum_{i=1}^{n} m_i + \sum_{i=1}^{n} d_{c_k(i)} \right)$

(5) Compute $M_k = R_k M + t_k$ and the root mean square error $D_k = \sqrt{\frac{1}{n} \sum_{i=1}^{n} \| m_i - d_{c_k(i)} \|^2}, m_i \in M_k$.

(6) Evaluate termination conditions: if $| D_k - D_{k-1} | < T_{\min}$ or the iteration limit is reached, stop the operation; otherwise, proceed to step 3. $T_{\min}$ is a predefined threshold.

The constraint ICP algorithm controls the rotation angle range in the process of point cloud registration to avoid deviation from the true value of rotation angle. It can effectively suppress the adverse effects of noise and low overlap ratio in the registration process, thus improving the applicability and accuracy of the algorithm.

3.2.3 Point Cloud Data Processing and 3D Modeling

This paper will center around Yudu County in the northeastern region of Ganzhou City in Jiangxi Province. Yudu was one of the essential elements of China's revolutionary bases and a place where seasoned proletarian revolutionaries carried out their magnificent revolutionary activities, as well as the sole county fully controlled by the Red Army just before the Long March. Thus, there is a considerable amount of red architecture in Yudu County. The

transformation of such architectural heritage to 3D models can facilitate further development of red heritage in the digital world. With the modeling procedures and techniques explained above, the process of modeling the red architectural heritage of Yudu County is as follows:

(1) Point cloud denoising and simplification. Load the point cloud data in Cloud Compare application and initially undertake its denoising and rough removal. By the "Crop" command, cut off all unrelated objects such as surrounding constructions, ground, trees, cars, and others from the red buildings heritage. Next, proceed to more accurate denoising of the buildings heritage. Conduct denoising of the point cloud data using the software commands, and then manually refine the process by removing extra points from the buildings. In case the point cloud data is excessively dense, conduct hierarchical thinning.

(2) Building Segmentation and Manual Point Cloud Completion. Remeasure and complete the red heritage building segmentation and perform manual completion for each separate building individually. Study the views from the front, sides, and top views, where there may be any holes. Use the general attributes of the red heritage buildings and photographs from the past to manually complete the holes in the point cloud.

(3) Building Contour Extraction and Segmentation. Using point cloud data after the substantial completion of each separate building, estimate the 2D contours in front view, side view, top view, and cross section views. It will lead us to get the contour line and elevation sketch of each building with centimeter level accuracy.

(4) 3D Model Construction. Import centimeter-level contour line and elevation sketches of buildings into Revit software and use point cloud data to create 3D models.

3.3 Verification of 3D Modeling Accuracy for Red Heritage Sites

3.3.1 Effectiveness of Point Cloud Thinning Algorithms

In the case of the generation of the 3D model for red heritage sites in Yudu County, decreasing the amount of the point cloud will result in increasing the accuracy of 3D models. Thus, there is an urgent need to study the performance of point cloud thinning algorithms. Therefore, this paper will make comparisons among Random Sampling (RS), Distance-Equidistant (DE), and our curvature-based thinning algorithm (Ours). In addition, the effectiveness of different thinning algorithms on different slopes and point cloud retention rates will be considered. RMSE of elevation will be used as the criterion of effectiveness. From 100 point clouds, we generate a DEM and take 15 checkpoints from each one for validation. The results are presented in Figure 4 and Table 2.

Generally speaking, as the thinning factor rises, i.e., the point cloud retention rate decreases, DEM error will rise gradually. With respect to the terrain slope, a positive relationship will be found between DEM error and the increase in slope. Among the three thinning methods, the curvature-based hierarchical thinning method demonstrates superior error suppression compared to the other two methods at steeper slopes. When terrain slope < 25°, although DEM accuracy shows a negative correlation with slope, the error increase is relatively slow with increasing slope. When slope exceeds 25°, DEM error increases significantly faster.

Furthermore, at slopes between 35° and 45°, even when retaining 85% of the original point cloud data, the RMSE of DEMs generated by any downsampling method remains high—approximately 4 to 5 times greater than that achieved at similar point cloud retention rates under low slopes (<15°). As the thinning ratio increases, the number of retained ground points gradually decreases, and the RMSE continuously increases. When the terrain slope is between 35° and 45° and the point cloud retention rate is only 15%, the RMSE peaks at 1.276, which is nearly 5.04 times that of the same point cloud retention rate at smaller terrain slopes (<15°). For larger terrain angles (25°–45°), especially when the terrain angle is between 35°–45°, the

curvature-based point cloud thinning technique proves itself to be the most effective one. With increasing point cloud thinning ratio, the accuracy gain of the curvature-based technique in comparison with the other two techniques increases significantly. At an angle range of 35°–45° and a point cloud thinning ratio of 45%, the curvature thinning technique can produce a result that is up to 0.22% more accurate than the other two thinning algorithms. In cases where the angle value is decreasing, the RMSE difference between the three thinning techniques becomes almost negligible, although the equidistant thinning algorithm proves slightly better at smaller angles. With a slope value lower than 15°, different point cloud thinning techniques do not affect DEM accuracy significantly; even with a thinning ratio of 15%, the RMSE does not exceed 0.253.

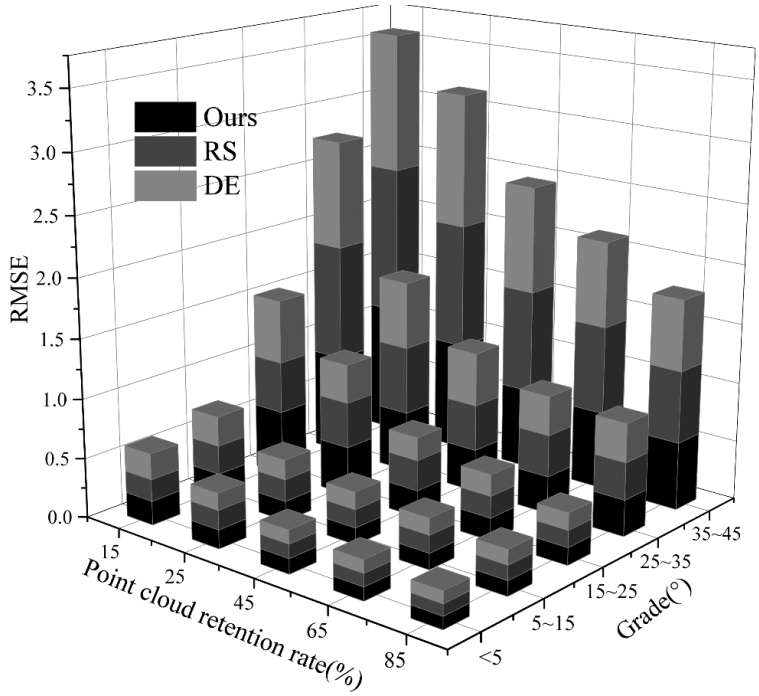

Figure 4: DEM elevation RMSE distribution

Table 2: RMSE of DEM results

Grade (°)	Algorithm	Point cloud retention rate				
		15%	25%	45%	65%	85%
<5	Ours	0.202	0.158	0.127	0.113	0.105
	RS	0.183	0.162	0.118	0.107	0.095
	DE	0.217	0.143	0.115	0.109	0.101
5~15	Ours	0.215	0.168	0.141	0.135	0.126
	RS	0.243	0.185	0.152	0.147	0.123
	DE	0.253	0.167	0.148	0.139	0.126
15~25	Ours	0.553	0.416	0.227	0.189	0.146
	RS	0.437	0.386	0.258	0.182	0.141
	DE	0.538	0.326	0.195	0.181	0.143
25~35	Ours	0.853	0.517	0.362	0.315	0.306
	RS	0.983	0.576	0.389	0.352	0.313
	DE	0.919	0.568	0.449	0.331	0.325
35~45	Ours	1.112	0.938	0.684	0.656	0.573

	RS	1.276	1.065	0.872	0.743	0.606
	DE	1.185	1.141	0.904	0.721	0.599

Besides, the features like steeper slopes, severe jittering, and many bubbles, among others, are found in the triangular mesh and contours resulting from the initial dataset of points. Moreover, there is a considerable amount of meaningless noise data. Even isolated points can trigger the appearance of contour lines. After applying a curvature-based hierarchical thinning algorithm to the point cloud data, the comparison results are shown in Figure 5, where Figure 5(a) and (b) represent the original contour lines and the thinned contour lines, respectively. As evident from the figures, the curvature-based hierarchical thinning algorithm significantly reduces noise in the generated DEM and contour line data, achieving an ideal effect of twice the result with half the effort. When applied to the 3D digital modeling of Jiangxi's red heritage sites, this approach ensures the accuracy of architectural outlines and elevation line drawings in the 3D models.

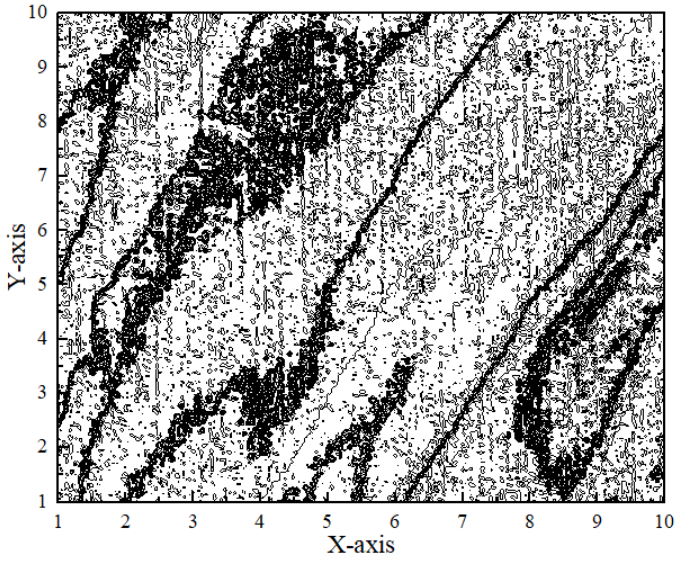

(a) Original contour line

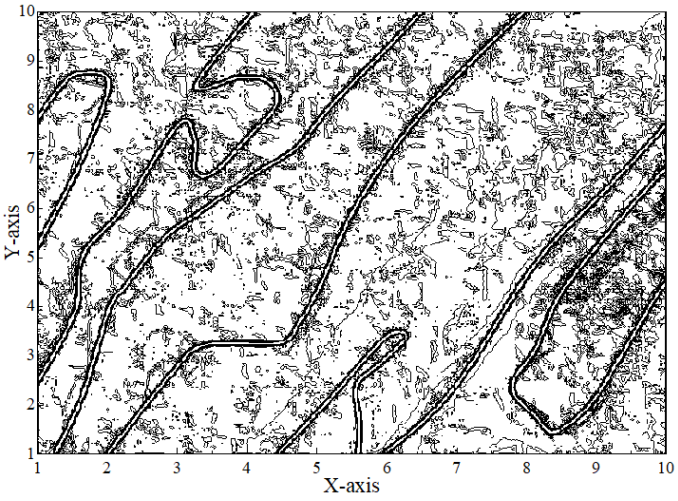

(b) Contour lines after thinning

Figure 5: Comparison of contour lines after dilution

3.3.2 Validation Analysis of Point Cloud Registration Methods

To validate the effectiveness of the proposed algorithm, this paper employs data acquired through UAV oblique measurement technology of Yudu County's red architectural heritage as input for the improved ICP algorithm with rotational angle constraints. The algorithm's results then serve as experimental data. Data set A primarily comprises point cloud data from various red architectural heritage sites in Yudu County. Data sets B–D correspond to the publicly available datasets Mulran Dataset KAIST, DDC, and Riverside, respectively.

Quantitative analysis was conducted by calculating the Root Mean Square Error (RMSE) of distances between matched keypoints from pre-optimized and post-optimized point clouds. The RMSE of matched point pairs served as the evaluation criterion to quantitatively analyze relative accuracy changes in segmented point clouds before and after optimization. For each edge in the iterative pose graph constructed from Data A and Data B, matched point pairs were identified via nearest neighbor search between the corresponding point clouds, followed by RMSE calculation. RMSE of average distance can be achieved by adding up all distance RMSEs and then dividing by the total number of edges. Table 3 represents the value of average distance RMSE of the matched point pairs before and after optimization.

It is clear from the above data that prior to the optimization process, the average distance RMSE of the matched point pairs was quite high, implying that there was an issue with rotational drift. Nevertheless, the proposed algorithm performed very well on this data set. For Data A, with optimization of rotation angle constraint error, the average distance RMSE of the matched point pairs was reduced from 2.681 m to 0.238 m. With coarse optimization, it was brought down to 0.174 m and through fine optimization to 0.156 m. This indicates a 94.18% improvement in the average RMSE from the pre-optimization stage. In the case of Data B, the average distance RMSE was decreased to 0.335m through rotation angle constraint error optimization. By coarse optimization, the average distance RMSE is decreased to 0.287m and even decreased to 0.216m through fine optimization, which means the RMSE decreased by 97.90%. The same pattern was seen for Data C and D, where the distance RMSE is 98.85% and 95.47% improved, respectively.

The experiment shows that the improved ICP point cloud registration algorithm under rotation angle constraints can improve the error of rotation angle drift and greatly decrease the distance RMSE of matched points in global matching of the obtained 3D point cloud data using UAV oblique photogrammetry. These findings validate the effectiveness and feasibility of the proposed optimization method.

Table 3: The average value of the distance RMSE of the matching point pairs (m)

Optimize the status	Data A	Data B	Data C	Data D
Before optimization	2.681	10.273	19.024	3.424
Rotation Angle constraint optimization	0.238	0.335	0.401	0.226
After rough optimization	0.174	0.287	0.345	0.198
After fine optimization	0.156	0.216	0.219	0.155

3.3.3 Analysis of 3D Model Modeling Accuracy

A realistic 3D model can be developed based on image processing of the data obtained via oblique photography technology. In this paper, the 3D model of Yudu County's red building heritage has been established and can be viewed using 3Dview. In this way, the 3D geographic coordinate values can be obtained directly by the 3D model. Under the assumption that the

RTK-measured coordinates of the control points can be regarded as true value coordinates, the measurement of the coordinate values at eight control points on the 3D model and the field measurement were compared. The results of the comparison are shown in Table 4. The maximum error of the plane coordinate (ΔX) of the 3D model point was 0.0177m, and the maximum elevation error (ΔZ) of the model point was 0.1336m. Overall, the approach utilized in this paper has achieved relatively high accuracy errors in the creation of a 3D model of Yudu County's red building heritage.

Table 4: Checkpoint coordinate comparison result (m)

-	X	Y	Z	X-Actual	Y-Actual	Z-Actual
1	3603515.79	501039.76	45.08	3603515.7851	501039.5732	45.1824
2	3603427.14	501211.92	46.73	3603427.1542	501211.8963	46.5964
3	3603554.95	501118.83	46.12	3603554.9601	501118.8547	46.1045
4	3603341.52	501210.05	45.56	3603341.5148	501210.0622	45.5458
5	3603358.46	501057.89	43.41	3603358.4547	501057.8851	43.4352
6	3603353.07	501206.01	44.27	3603353.0802	501206.0167	44.2836
7	3603591.68	501089.63	43.22	3603591.6795	501089.6253	43.2015
8	3603338.53	501046.57	46.59	3603338.5123	501046.5892	46.5874

In addition to that, an investigation was carried out regarding the accuracy of the corner point coordinates in the 3D model of the red architectural heritage of Yudu County, which was created by this research study, to check whether the accuracy of the coordinates matches the specifications and requirements for large-scale surveying. Eight corner point coordinates were examined for their accuracies through field measurement of corresponding coordinates on the 3D model using a total station. After calculating the difference between the field measurement results and the coordinates on the 3D model, the analysis is provided in Table 5, where the errors in the corner point coordinates are demonstrated.

From the above data, one can see that the mean errors of coordinates in the X and Y directions are 0.012m and 0.048m, respectively, and the average error of coordinate is 0.024m. For digital mapping at the 1:500 scale, the mean error of coordinates in all directions must be below 0.15m, and the requirement is met in this case. Hence, it can be concluded that the 3D model of the red construction heritage of Yudu County, created in this research, is highly accurate. As a 3D resource for teaching, it will help students understand building structure.

Table 5: The corner error results of 3D model buildings (m)

	Actual coordinates		Model coordinates		Residual		
	X	Y	X	Y	ΔX	ΔY	ΔXY
1	***110.513	***694.156	***110.524	***694.163	-0.011	-0.007	0.0121
2	***108.877	***633.645	***108.851	***633.652	0.026	-0.007	0.0143
3	***105.364	***511.597	***105.372	***512.604	-0.008	-1.007	0.0159
4	***238.526	***528.262	***238.528	***528.271	-0.002	-0.009	0.0204
5	***216.918	***483.876	***216.924	***483.869	-0.006	0.007	0.0231
6	***224.372	***776.343	***224.369	***776.349	0.003	-0.006	0.0288
7	***208.514	***776.514	***208.507	***776.528	0.007	-0.014	0.0183
8	***021.753	***812.486	***021.761	***812.494	-0.008	-0.008	0.0223
Mean error					0.012	0.048	0.024

4 Engineering Cost Teaching Supported by Three-Dimensional Models of Red Heritage Sites

The traditional teaching modes of engineering cost classes are limited by many aspects like the capacity of the physical training laboratory, the equipment, and the financial investment, which leads to low teaching resource utilization. In the wake of the continuous rise of online education websites, the benefits brought by these online education websites are far more than those of traditional ones. They not only have the ability to provide all kinds of excellent teaching resources but also construct the 3D models of red construction heritage. This allows students to have a comprehensive understanding of these heritage sites' structures and thus perform precise engineering cost management.

4.1 Research Subjects and Teaching Methodology Design

4.1.1 Research Subjects and Teaching Resources

(1) Selection of Teaching Subjects

Students in the Engineering Cost major of L University became the target subjects of this investigation; Class 1 and Class 2 of the major were used as subjects. Specifically, Class 1 became the control group under the traditional teaching method, while Class 2 became the experimental group under the online education model. Baseline tests were performed on all subjects in the two classes. Both classes had equal number of 50 students and same ratios of male and female genders. The subjects in both classes showed similar entrance test scores and level of academic proficiency. During the initial process of learning, the subjects in both classes experienced equal instruction material, environments, and teachers. This ensured objectivity of the research data.

Teaching Practice Period: From March to July 2024. The students in both classes were tested before and after the experiment.

(2) Selection of Teaching Resources Online teaching resources are plentiful, varied, and appealing. Educators can create customized digital educational materials based on their courses to arouse the learners' enthusiasm and interest. The primary online educational resources comprise multimedia presentations, MOOC videos, 3D models, photos, mind maps, exercise questions, and practical projects. They are published in the online platform for easy access by students. Out of the above resources, the 3D models contain the "Red Construction Heritage Model of Yudu County, Jiangxi Province". This 3D model helps learners comprehend the architecture structure during the revolutionary period, which contributes to innovative designs and engineering costs calculation. Teachers need to make appropriate online teaching resources, design them differently, arrange them properly, be concise and relevant in terms of content, set proper task difficulty, and focus on interests and exemplary qualities.

4.1.2 Practical Teaching Methods for Engineering Cost Estimation

In practical teaching regarding the engineering cost course discussed in this paper, the control class used the conventional teaching method while the experiment group used the following approaches:

(1) Before the start of the course, students were divided into groups to tour the surveying laboratory. The surveying laboratory was created collaboratively with organizations where students could see the layout and mechanism of instruments. Thus, they gained an initial idea about surveying tools, creating a basis for further practical training. While teaching, all resources provided by the online learning system were utilized. Learning materials, such as

lecture notes and experiment videos, were provided prior to classes to prepare in advance, and this would be included in their performance evaluation. After classes, important concepts and difficult topics would be published to enhance learning.

(2) To facilitate seamless practical teaching, teachers offered specialized training on how to use the 3D modeling software to group leaders in advance. Meanwhile, other learners were given a glimpse of the software application process and laboratory working procedures through instructional videos and experiment explanations via the lab's teaching website. On this basis, a training model of "on-site faculty guidance + group leader demonstration + intra-group cooperation" was adopted. This involved: - Hands-on practical guidance by faculty members - Pre-learning and leadership by group leaders in team activities - Discussion within groups - Self-directed learning in the laboratory after class Such a comprehensive mode of operation promotes interaction between teachers, group leaders, and members, thereby increasing teaching efficiency. Additionally, the discussion of practical cases inspires students to share their insights. Through the analysis of case examples of 3D models of construction sites of the red heritage, students gain analytical and problem-solving abilities.

(3) In the experiment, concrete tasks are formulated with respect to the content of the measurement practice. For angular measurement practice, students have to measure the interior angles of polygons. As far as leveling measurement practice is concerned, students have to make surveys of closed leveling paths. Students are instructed to perform surveys and layout of building pile foundation centerlines in accordance with the blueprint in total station measurement practice. The course includes both virtual and practical work using the virtual software from Southern Surveying to help students create 3D drawings of buildings.

4.1.3 Student Learning Effectiveness Survey Questionnaire

In order to find out students' satisfaction level towards blended learning strategies, taking into account their satisfaction level about the design of instruction and learning models, an effective teaching questionnaire for the Engineering Cost class was designed. The questionnaire covers three aspects: student's satisfaction with the instructional content and methodology of blended learning, student's learning achievement through blended learning, and experiences of the student through the learning process. The five-point scale of measurement was used, namely "Strongly Agree," "Somewhat Agree," "Neutral," "Somewhat Disagree," and "Strongly Disagree." The questionnaire content is shown in Table 6.

Table 6: Questionnaire on Students' Learning Outcomes

Dimension	Survey item	Code
Teaching resources	Online learning resource satisfaction	XX1
	Course resource recognition	XX2
	Class interaction frequency	XX3
	Learning platform satisfaction	XX4
Teaching effect	Problem solving	XX5
	Team ability	XX6
	Verbal ability	XX7
	Ability to comb	XX8
Overall satisfaction	Overall course satisfaction	XX9
	Willing to use mixed teaching	XX10

After the end of teaching practices, questionnaires were distributed among all 50 participants of the experimental class. The total number of respondents was obtained, and the response rate of 100% was reached. Before analyzing the data from the questionnaire, we performed reliability and validity analysis using the software SPSS. Based on the results of reliability and validity analysis, the reliability coefficient α in our study is equal to 0.971, which shows that the test questions have high reliability and research results can be generalized. The validity index KMO is 0.908, while the significance level is below 0.01. Thus, the questions of our questionnaire effectively demonstrate their construct. The significance level of the questionnaire is lower than 0.05, which confirms its good construct validity and appropriateness for further factor analysis.

4.2 Practical Outcomes of the Construction Cost Estimation Course

4.2.1 Comparative Analysis of Student Course Grades

Formative assessments of the experimental class students mostly concentrate on their progress in online learning, participation in the classroom, and submission of assignments. On the other hand, formative assessments of the control class students largely concentrate on the rate of attendance, their performance on a daily basis, and assignment submission. The data obtained from the experiment after the first semester of instruction is presented below in Figure 6.

As seen in the graph, blended learning offers a much more versatile, personalized, and diversified learning experience for learners. This can help in stimulating their interest in learning, improving their participation in the classroom setting, and increasing their motivation. As a result, learners in the experimental group were able to perform better than their counterparts in the control group during formative assessments, especially in scoring higher marks (91-100 points). This is an indication of their strong learning abilities and deep understanding of the course content, which was made possible by the application of the blended learning technique. On the other hand, the learners in the control group performed poorly, especially in scoring higher marks (91-100 points).

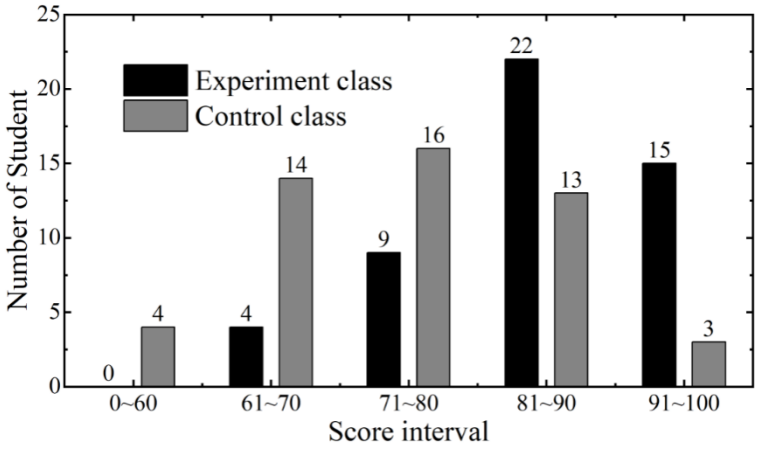

Figure 6: The distribution of students' exam scores across various score ranges

After the completion of the teaching semester, both experimental and control groups were simultaneously assessed using equivalent examination papers. The statistics regarding the distribution of scores from both groups are shown in Fig. 7. The analysis of the data provided suggests that despite the presence of similarities in the patterns of summative assessment score distribution, the experimental group scored better than the control group concerning the rate of excellent scores, good scores, and pass scores. Moreover, the number of students from the experimental group achieving scores over 81 points was slightly higher than that of the students from the control group, with an even higher rate in the range of 71-80 points. Through comparative assessment of the data obtained from formative and summative assessments, it is apparent that the experimental group scored better on average than the control group in terms of average scores, excellent scores, and pass scores. In general, the students in the experimental group performed better than those in the control group, thus proving the effectiveness of the blended teaching technique. It seems to be more effective in arousing interest in learning among the students and promoting self-study skills.

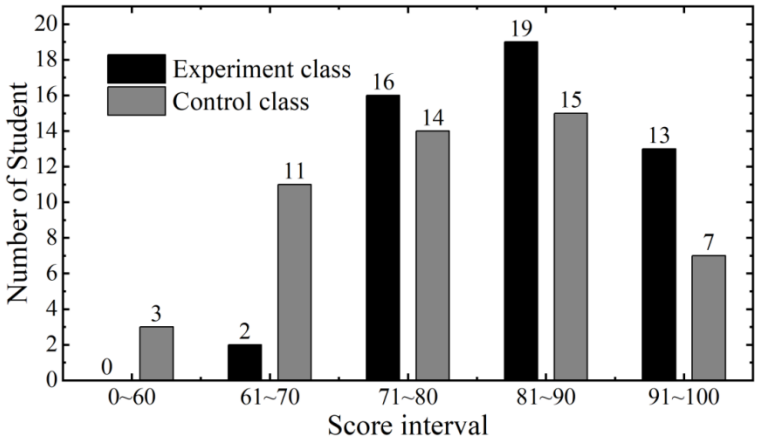

Figure 7: The statistics of the score ranges for the two classes

4.2.2 Survey Results on Student Learning Outcomes

To improve the teaching quality of engineering cost courses and to assess the practicality of the blended learning model using the 3D model of Yudu County's red construction heritage, the satisfaction survey has been carried out. This questionnaire included questions pertaining to three main aspects such as teaching resources, teaching effectiveness, and satisfaction. After

combining student questionnaires, valid responses have been analyzed, and the survey result on student academic achievement is shown in Figure 8 below.

From the graph, it can be seen that 85% of the students are satisfied with the course resources provided online. As far as resource recognition is concerned, over 80% of the students felt that the resources assisted them in understanding course content better. In case of active participation, around 80% of students stated that they were actively involved in course interaction sessions. Also, over 70.51% were satisfied with the online learning environment. Student satisfaction regarding the teaching resources is quite high. 81.98% reported improved abilities to solve problems, work in a team, and verbal communication, whereas 79.42% showed enhanced knowledge structuring and mathematical reasoning capabilities. Yet, 20% of the students continue to have difficulties in the design, implementation, and operation stage. They struggle to design and optimize architectural 3D models according to instructor guidance, resulting in limited professional skill development. Instructors should prioritize strengthening personalized guidance during the teaching process. Overall, students achieved good learning outcomes across the conceptualization, design, implementation, and operation phases, indirectly demonstrating that blended learning facilitates the development of students' professional competencies. Furthermore, students expressed high satisfaction with the blended learning approach integrating 3D models of Jiangxi's red construction heritage. 96.67% of students reported overall satisfaction with the course, and over 85% indicated willingness for instructors to continue using blended learning models in future teaching.

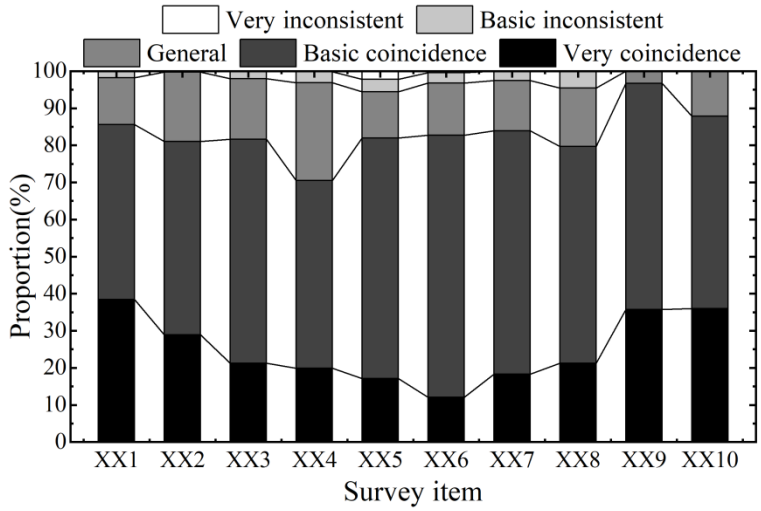

Figure 8: The survey and statistical results of students' learning outcomes

5 Conclusion

This article establishes a digital transformation framework for Jiangxi's red architectural heritage from dual perspectives of historical cost and modern technology, integrating the quadruple helix theory. It proposes a transformation pathway for applying this framework to engineering cost course instruction. Taking the red construction heritage in Yudu County as the research subject, the study employed drone oblique measurement technology to acquire three-dimensional data. By integrating point cloud thinning and registration algorithms, a 3D model of the red construction heritage was constructed and uploaded to an online teaching platform as educational resources, thereby aiding students in better understanding architectural structures. From the practice of the teaching method, it is evident that the model of learning using the integration of the 3D models plays an important role in improving student learning and

achieving high performance levels. In addition, using the integration of history and technology to digitize the red construction heritage of Jiangxi province creates rich teaching resources. This not only achieves innovative utilization of red construction heritage but also offers a novel method for elevating the quality of engineering cost course instruction.

Funding

This work was supported by "Crafting Dreams with Expertise": A Study on Innovative Approaches to Integrating Jiangxi's Revolutionary Construction History into Construction Cost Engineering Curricula (Project No.: HSWH25110).

About the Author

Jianjing Zhou was born in Nanchang City, Jiangxi Province, China in 1981. He obtained a Master's degree from Nanchang University. He is currently teaching at the College of Modern Economics & Management, JUFE, with a primary research focus on engineering project management.

Liyuan Wang was born in Nanchang City, Jiangxi Province, China in 1983. She obtained her PhD degree from Coventry University, UK. She is currently teaching at the Foreign Languages School, Jiangxi University of Finance and Economics, with a primary research focus on higher education.

Liyuan Wang is the corresponding author of this paper

References

[1] Kaili, H., & BoYuan, S. (2022, January). Conservation and Inheritance of Gansu Red Architectural Cultural Heritage from the Perspective of Landscape Anthropology. In 2021 International Conference on Public Art and Human Development (ICPAHD 2021) (pp. 216-219). Atlantis Press.

[2] Dong, H. A. N., Meng, L. I., Xiaoyuan, H. A. O., & Li, H. A. N. (2019). Tourists' Perception of Celebrity Memorial Hall Under Red Tourism Back-ground: A Case Study of Wu Lanfu Memorial Hall. Journal of Landscape Research, 11(4).

[3] Chawla, M. I. (2025). Chinese Revolutionary Heritage: Exploring Revolutionary Culture in Huanggang. Annals of Human and Social Sciences, 6(3), 51-60.

[4] Barnes, A. J. (2018). Representing the China Dream: A case study in revolutionary cultural heritage. In A Museum Studies Approach to Heritage (pp. 797-813). Routledge.

[5] Wang, Y., Chun, Q., Xiong, X., & Zhu, T. (2022). Conservation and adaptive reuse of modern military industrial heritage: a case study on the former site of Jinling Arsenal in Nanjing, China. Journal of Asian Architecture and Building Engineering, 21(4), 1193-1210.

[6] Chen, M., Zhao, B., Zhao, H., Jiang, Q., Zhou, Q., & Tong, H. (2023). Character-defining elements comparison and heritage regeneration for the former command posts of the Jinan campaign—A case of Chinese rural revolutionary heritage. Buildings, 13(8), 1923.

[7] Zhu, Y., Xu, F., Wei, W., & Wang, R. (2023). Research on Protection and Inheritance of Red Revolutionary Buildings--A Case Study of Geyuan Town, Hengfeng County, Jiangxi Province. In SHS Web of Conferences (Vol. 152, p. 02003). EDP Sciences.

[8] Mykytyuk, Y. (2024). Evaluation and management of the cost of investment and construction projects. Herald of Economics, (2), 226-237.

[9] Fu, Y., Zhou, J., & Zhang, J. (2023). Construction of four-dimensional practical teaching system for engineering cost specialty in vocational colleges. International Journal of New Developments in Education, 5(9).

[10] Albu, S. (2021). The Economic Value and Valuation of Architectural Heritage. Journal of Building Construction and Planning Research.

[11] Abdelrazek, H., & Yılmaz, Y. (2020). Methodology toward cost-optimal and energy-efficient retrofitting of historic buildings. Journal of Architectural Engineering, 26(4), 05020009.

[12] Falcào Silva, M. J., Salvado, F., & Baiào, M. (2017). ARCHITECTURAL HERITAGE SUSTAINABLE REHABILITATION: PROPOSAL FOR APPLICATION OF COST-BENEFIT ANALYSIS. International Journal for Housing Science & Its Applications, 41(2).

[13] Ramos, J. S., Domínguez, S. Á., Moreno, M. P., Delgado, M. G., Rodríguez, L. R., & Ríos, J. A. T. (2019). Design of the refurbishment of historic buildings with a cost-optimal methodology: A case study. Applied Sciences, 9(15), 3104.

[14] Guner, A. F., & Benli, G. (2019). Project management in conservation and restoration of historic buildings. SAR J, 2, 24-30.

[15] Jordan-Palomar, I., Tzortzopoulos, P., García-Valldecabres, J., & Pellicer, E. (2018). Protocol to manage heritage-building interventions using heritage building information modelling (HBIM). Sustainability, 10(4), 908.

[16] Maselli, G., Cucco, P., Nesticò, A., & Ribera, F. (2024). Historical heritage–MultiCriteria Decision Method (H-MCDM) to prioritize intervention strategies for the adaptive reuse of valuable architectural assets. MethodsX, 12, 102487.

[17] Ben Charif, H., Zerlenga, O., & Iaderosa, R. (2024). Low-Cost Photogrammetry for Detailed Documentation and Condition Assessment of Earthen Architectural Heritage: The Ex-Hotel Oasis Rouge in Timimoun as a Case Study. Buildings (2075-5309), 14(10).

[18] Hao, Y., Yao, Z., Wu, R., & Bao, Y. (2024). Damage and restoration technology of historic buildings of brick and wood structures: a review. Heritage Science, 12(1), 301.

[19] Lele Ye, Hui Lin & Xiaogang Chen. (2024). Narrative Design of Red Cultural Heritage Landscape in Jiangxi Province—Take Fang Zhimin Martyrs' Memorial Park as An Example. Journal of Research in Science and Engineering, 6(5).

[20] Shangming Wu, Lin Feng, Xiaorui Zhang, Chaoen Yin, Lei Quan & Bo Tian. (2025). Optimizing overlap percentage for enhanced accuracy and efficiency in oblique

photogrammetry building 3D modeling. Construction and Building Materials, 489, 142382-142382.

[21] Cheng Wang,Chenglu Wen,Yudi Dai,Shangshu Yu & Minghao Liu. (2020). Urban 3D modeling with mobile laser scanning: a review. Virtual Reality & Intelligent Hardware, 2(3),175-212.